Local exposure of phosphatidylethanolamine on the yeast plasma membrane is implicated in cell polarity

Kunihiko Iwamoto[1], Shingo Kobayashi[1], Ryouichi Fukuda[1], Masato Umeda[2], Toshihide Kobayashi[3] and Akinori Ohta[1,*]

[1]*Department of Biotechnology, The University of Tokyo, 1-1-1 Yayoi, Bunkyo-ku, Tokyo 113-8657, Japan*
[2]*Institute for Chemical Research, Kyoto University, Gokajo, Uji-shi, Kyoto 611-0011, Japan*
[3]*Frontier Research System, RIKEN (Institute of Physical and Chemical Research), 2-1 Hirosawa, Wako-shi, Saitama 351-0198, Japan*

Cell surface phosphatidylethanolamine (PE) of the yeast cell was probed by biotinylated Ro09-0198 (Bio-Ro), which specifically binds to PE and was visualized with fluorescein-labelled streptavidin. In *Saccharomyces cerevisiae*, the signals were observed at the presumptive bud site, the emerging small bud cortex, the bud neck of the late mitotic large-budded cells and the tip of the mating projection. In *Schizosaccharomyces pombe*, the signals were observed at one end or both ends of mono-nucleated cells and the division plane of the late mitotic cells. These sites were polarized ends in the yeast cells, implying that PE is exposed on the cell surface at cellular polarized ends. Treatment of *S. cerevisiae* cells with Ro09-0198 resulted in aberrant F-actin accumulation at the above sites, implying that limited surface exposure of PE is involved in the polarized organization of the actin cytoskeleton. Furthermore, *S. cerevisiae ros3*, *dnf1* and *dnf2* null mutants, which were known to be defective in the internalization of fluorescence-labelled PE, as well as the combinatorial mutants, were stained with Bio-Ro at the enlarging bud cortex, in addition to the Bio-Ro-staining sites of wild-type cells, suggesting that Ros3p, Dnf1p and Dnf2p are involved in the retrieval of exposed PE at the bud cortex.

Introduction

In the eukaryotic membrane, phosphatidylethanolamine (PE) is a ubiquitous phospholipid that has peculiar functions. It provides phosphoethanolamine to the junction between extracellular proteins and the glycosylphosphatidylinositol (GPI) anchor (Menon & Stevens 1992) and it is directly involved in an autophagic process (Ichimura *et al*. 2000; Kirisako *et al*. 2000). Furthermore, as it has a small polar head group, PE can form non-bilayer structures under physiological conditions. It is conceivable that the proportion of such non-bilayer-forming lipids contributes to the physical properties of the membrane, including membrane curvature (Dowhan 1997). PE is also a constituent of the plasma membrane and is believed to mainly reside in the inner leaflet of its bilayer structure in a wide variety of mammalian cells (Zachowski 1993). This asymmetric distribution is thought to be maintained by ATP-dependent lipid translocators in the eukaryotic cells (Zachowski 1993; Bevers *et al*. 1999; Grant *et al*. 2001; Daleke 2003). However, the actual distribution of PE in the plasma membrane and its roles in cell activity have not yet been fully explored, probably because of the lack of a tool to visually distinguish surface PE from the bulk of cellular PE.

The antibiotic Ro09-0198 (Ro, cinnamycin) is a tetracyclic polypeptide of 19 amino acids (Kessler *et al*. 1988). Ro specifically binds to PE on the surface of liposomes or mammalian cells, but does not bind to other phospholipids such as phosphatidylcholine (PC), phosphatidylserine (PS) and sphingomyelin. In addition, Ro causes leakage of the contents of liposomes and leads to the cytolysis of mammalian cells (Choung *et al*. 1988a,b; Makino *et al*. 2003). While amino-terminal biotinylated Ro (Bio-Ro) possesses almost the same properties as Ro (Aoki *et al*. 1994), the fluorescein-labelled streptavidin (FITC-SA)-conjugated Bio-Ro (FL-SA-Ro) retains its specific PE-binding ability, but does not lead to the cytolysis of mammalian cells (Emoto *et al*. 1996). Therefore, Ro and its derivatives should be specific probes to detect PE on the cell surface. Emoto and colleagues used FL-SA-Ro to analyse the distribution of PE in the plasma membrane of Chinese hamster ovary (CHO) cells. They found that this probe specifically bound at the cleavage furrow of dividing cells and it also inhibited cytokinesis at the stage of contractile ring disassembly (Emoto *et al*. 1996; Emoto

Communicated by: Yoshinori Ohsumi
**Correspondence*: E-mail: aaohta@mail.ecc.u-tokyo.ac.jp

DOI: 10.1111/j.1365-2443.2004.00782.x

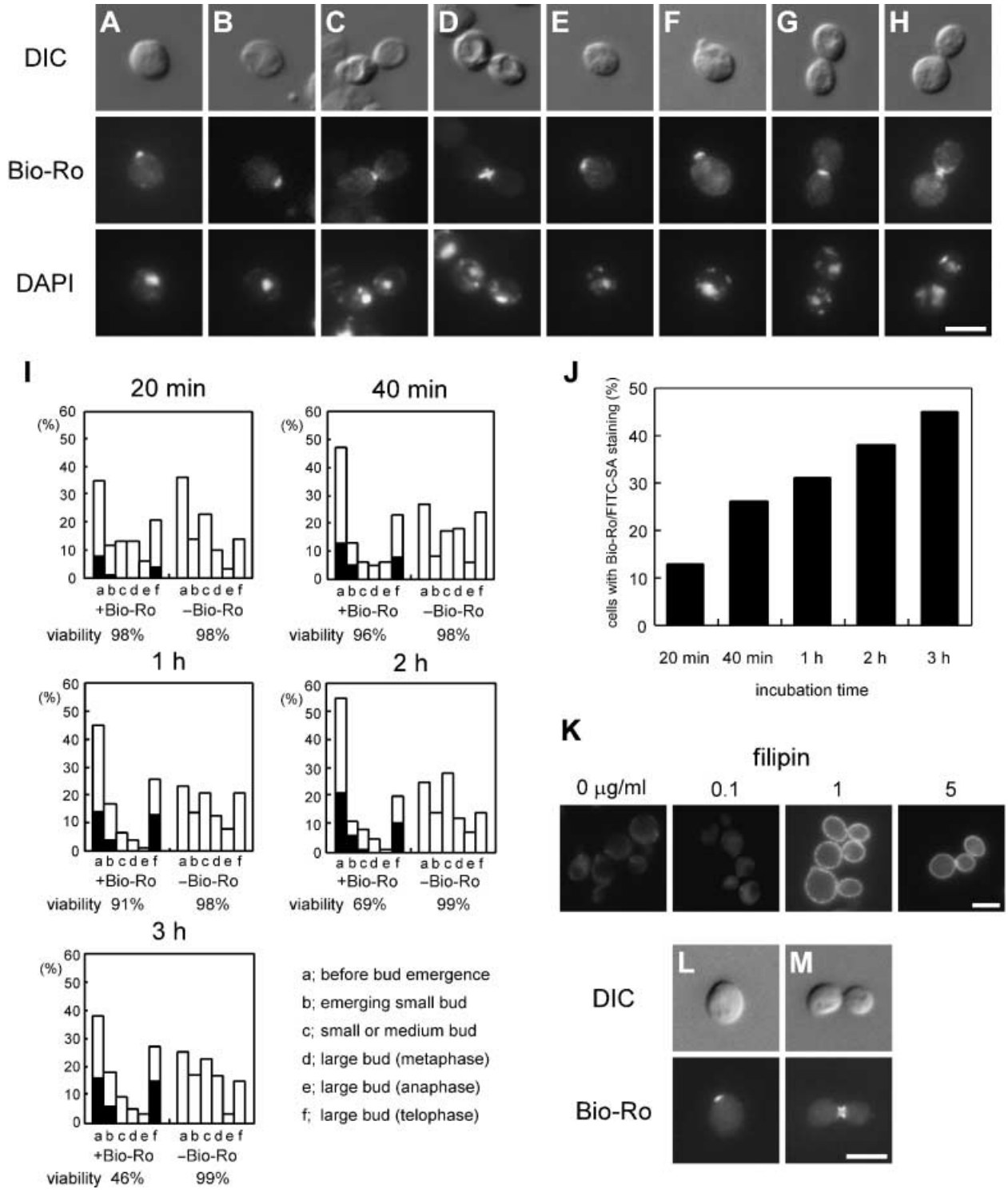

Figure 1 Budding yeast cells were stained with Bio-Ro at specific sites on the plasma membrane during specific stages of the cell cycle. (A–H) Exponentially growing budding yeast wild-type (W3031A) cells were treated with 100 μM Bio-Ro for 20 min (A–D) or 3 h (E–H). After fixation, the spheroplasts were incubated with DAPI and FITC-SA as described in Experimental procedures. Each panel contains a differential interference contrast (DIC) image (upper), a Bio-Ro/FITC-SA staining image (middle) and a DAPI staining image (lower). Bar, 5 μm (I,J) Exponentially growing W3031A cells were incubated with 100 μM Bio-Ro (+Bio-Ro) or without Bio-Ro

& Umeda 2000). These results strongly suggest that PE, which usually resides in the inner leaflet of the plasma membrane, is exposed on the surface of the plasma membrane at the cleavage furrow and is involved in the critical step of cytokinesis.

In budding yeast *Saccharomyces cerevisiae*, PE is essential for growth and this requirement of PE is considered to be independent of its non-bilayer-forming ability (Birner *et al*. 2001; Storey *et al*. 2001). Some proteins are known to be involved in the transbilayer translocation of PE across the plasma membrane by the internalization assay of fluorescence-labelled phospholipids. While Pdr5p and Yor1p, the members of ATP-binding cassette (ABC) transporters, were reported to contribute to the outward-directed PE translocation across the plasma membrane (Decottignies *et al*. 1998), Ros3p and two P-type ATPases, Dnf1p and Dnf2p, were reported to participate in the inward-directed PE translocation (Kato *et al*. 2002; Pomorski *et al*. 2003). *ROS3* was identified as a gene responsible for the Ro sensitivity in one of the Ro-sensitive *S. cerevisiae* mutants (Kato *et al*. 2002). Ros3p is an evolutionarily conserved protein and has two putative transmembrane domains. It was reported that Ros3p localized in the plasma membrane and the endoplasmic reticulum, and was involved in the internalization of fluorescence-labelled PE and PC (Kato *et al*. 2002). However, there is no significant homology between Ros3p and ABC transporters or P-type ATPases (Kato *et al*. 2002). Dnf1p and Dnf2p were also reported to primarily reside in the plasma membrane and be important for the internalization of fluorescence-labelled PE, PS and PC in *S. cerevisiae* (Pomorski *et al*. 2003).

Here, we developed a protocol for staining PE in the outer leaflet of the plasma membrane in *S. cerevisiae* and fission yeast *Schizosaccharomyces pombe* with Bio-Ro and FITC-SA. The signals were observed at the bud neck of the *S. cerevisiae* late mitotic large-budded cells and at the division plane of the *Sc. pombe* late mitotic cells, suggesting that PE exposure at the cell division site is widespread among eukaryotes. In addition to those at the cell division site, the signals were observed at the presumptive bud site, at the emerging small bud cortex and at the tip of the mating projection in *S. cerevisiae*, and at growing cell ends in *Sc. pombe*. These sites are polarized ends where actin patches accumulate and actin cables converge (Pruyne & Bretscher 2000a,b; Yarm *et al*. 2001; Nelson 2003). Therefore, our results suggest that PE is generally exposed on the cell surface at cellular polarized ends, including at the cell division site. When we treated *S. cerevisiae* cells with Ro to entrap surface-exposed PE, aberrant F-actin accumulation was observed at those sites. Therefore, limited surface PE exposure is likely to be involved in actin cytoskeleton organization and cell polarity.

As the fluorescence signals were observed during a limited period of the cell cycle in *S. cerevisiae* cells, exposed PE should be retrieved from the cell surface thereafter. *S. cerevisiae* mutants with *ros3*, *dnf1* or *dnf2* null mutation singly or in combination were stained with Bio-Ro at the enlarging bud cortex (i.e. the bud cortex of the small-, medium- and large-budded cells), in addition to the sites at which wild-type cells were stained with Bio-Ro. Thus, Ros3p, Dnf1p and Dnf2p are likely to be involved in the retrieval of exposed PE at the enlarging bud cortex after the initial stage of bud emergence.

Results

Bio-Ro/FITC-SA staining was observed at specific sites during specific stages of the cell cycle

To examine the distribution of Ro-binding sites on the plasma membrane in yeast, we treated exponentially growing *S. cerevisiae* cells with Bio-Ro for various time periods and visualized the bound Bio-Ro with FITC-SA after cell fixation (hereafter, 'Bio-Ro/FITC-SA staining'), as described in Experimental procedures. FL-SA-Ro was not directly used because FL-SA-Ro was too large to penetrate the yeast cell wall. When cells were treated with Bio-Ro for 20 min, the fluorescence signals were detected on the plasma membrane at the presumptive bud site (Fig. 1A,B), at the emerging small bud cortex (data not shown) and at the bud neck of the large-budded cells

(–Bio-Ro) for various periods. The percentages of the cells belong to the indicated categories were shown in (I) (n = 100). The categories were judged by a ratio of long axis length of bud to that of mother. A cell of which the ratio is less than 0.05 was defined as 'before bud emergence', between 0.05 and 0.25 as 'emerging small bud', between 0.25 and 0.55 as 'small or medium bud' and more than 0.55 as 'large bud'. Large bud with no nuclei (metaphase), with dividing nuclei (anaphase) and with divided nucleus (telophase) (Heald & Walczak 1999) were judged by DAPI staining. The percentages of the cells that had Bio-Ro/FITC-SA staining are also shown in black bar (I). Cell viability was measured by phloxine B staining as described in Experimental procedures. Data represent the percentages of viable cells out of about 10 000 cells (I). The percentages of the Bio-Ro-treated cells that had Bio-Ro/FITC-SA staining are shown in (J) (n = 100). (K) Exponentially growing W3031A cells were incubated with various concentrations of filipin (Sigma) for 15 min. Bar, 5 μm (L,M) Exponentially growing W3031A cells were treated with 100 μM Bio-Ro for 3 h at 4 °C. A DIC image (upper) and a Bio-Ro/FITC-SA staining image (lower) were obtained as described in (A–H). Bar, 5 μm.

(Fig. 1C,D). In some cases, Bio-Ro/FITC-SA staining at the bud neck was separated into the mother and daughter cells (Fig. 1D). These fluorescence signals were dependent on Bio-Ro treatment (Fig. 1I) and the staining pattern was not changed by the prolonged Bio-Ro treatment until at least 3 h (Fig. 1E–I). The population of the cells with Bio-Ro/FITC-SA staining increased with the time of Bio-Ro treatment and reached 45% of the total observed cells after 3 h (Fig. 1I,J). Living cell population was 98% and 96% of the total cell number after 20- and 40-min incubations with Bio-Ro, respectively, and then started to decline to 91%, 69% and 46% after 1-, 2- and 3-h incubations, respectively (Fig. 1I). After the 40-min incubation, Bio-Ro/FITC-SA-stained cells occupied 26% of the total cell number (Fig. 1J). These results strongly suggest that localized Bio-Ro/FITC-SA staining is reflecting local PE exposure on living yeast cells. We thereafter treated yeast cells with Bio-Ro for 3 h to effectively observe distribution of cell surface PE. When cells were treated with high and low concentrations of filipin that binds sterol, its fluorescence signals were not particularly limited to the sites where Bio-Ro bound (Fig. 1K), suggesting that the localized Bio-Ro/FITC-SA staining is not as a result of high permeability of the nearby cell wall.

Bio-Ro/FITC-SA staining seemed to be restricted to the cells in peculiar stages in the cell division cycle, i.e. cells without apparent bud but probably under the process of bud emergence (at the presumptive bud sites, Fig. 1A,B,E), cells with emerging small bud (at the emerging small bud cortex, Fig. 1F) and cells of which nuclear segregation was completed (at the bud neck, Fig. 1C,D,G,H). It is noteworthy that, after the addition of Bio-Ro, cells in categories c, d and e in Fig. 1(I) were decreased in their population whereas cells in categories a and f were not (Fig. 1I). In addition, the ratios of Bio-Ro/FITC-SA-stained cells in these two categories were elevated during Bio-Ro treatment (Fig. 1I). These results suggest that the progress of the cell division cycle was arrested by Bio-Ro treatment at the early stage of bud emergence or at the stage of cytokinesis. When cells were treated with hydroxyurea or nocodazole, which arrests cells in the S phase or mitotic metaphase, respectively, and then treated with Bio-Ro, fluorescence signals were not detected at the bud neck of the arrested large-budded cells (Fig. 2A), suggesting that PE is exposed at the bud neck after metaphase. This notion was further supported by a more detailed examination on the population of cells with large bud in a Bio-Ro-treated culture. The cells with Bio-Ro/FITC-SA staining at the bud neck were only observed among telophase population (Table 1). It is also noteworthy that the telophase population was increased to 85.3% during the 3-h

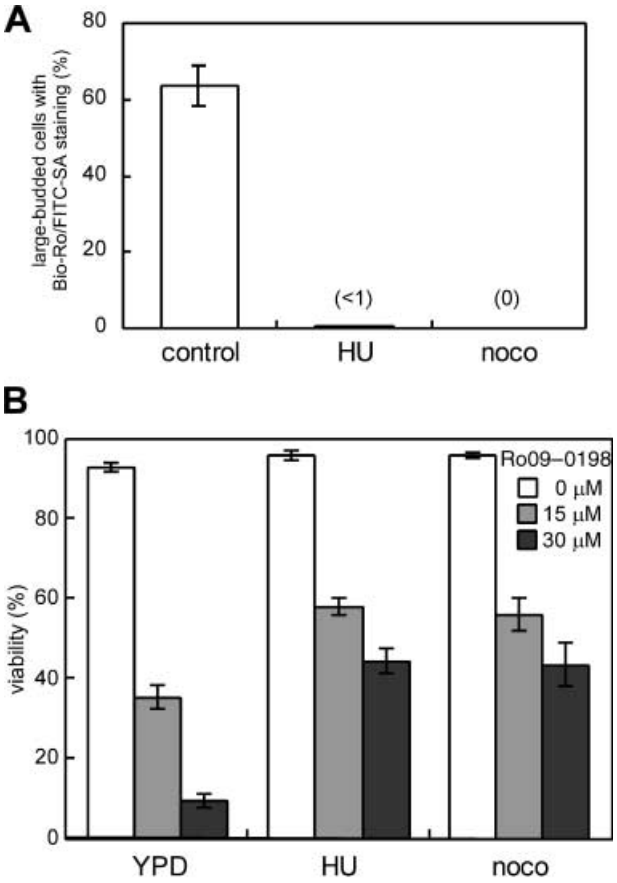

Figure 2 The large-budded cells arrested by hydroxyurea and nocodazole were not stained with Bio-Ro/FITC-SA. (A) Exponentially growing budding yeast wild-type (W3031A) cells were treated with 0.1 M hydroxyurea (ICN Biomedicals Inc.) or 15 μg/mL nocodazole (Sigma) for 3 h. The cells were then harvested, suspended in YPD medium containing Bio-Ro and hydroxyurea or nocodazole and incubated for an additional 3 h. The ratios of the cells with Bio-Ro/FITC-SA staining at the bud neck in large-budded cells are shown. The results represent means ± SEM values from three independent experiments (n = 100). (B) After the 3-h incubation with hydroxyurea or nocodazole as in (A), Ro was added at the final concentration of 0, 15 or 30 μM and the cells were further incubated for 3 h. After incubation with Ro, cell viability was measured by phloxine B staining as described in Experimental procedures. Although Ro was reported to possess the same PE-binding and haemolytic activity as Bio-Ro (Aoki *et al.* 1994), Ro is more effective in killing yeast cells, probably because of its lower permeability through the cell wall. Data represent the percentages of viable cells out of about 20 000 cells and values are means ± SEM from three independent experiments. Control, no treatment; HU, hydroxyurea treatment; noco, nocodazole treatment.

Table 1 Large-budded cells with Bio-Ro/FITC-SA staining at the bud neck had segregated nuclei

	Metaphase	Anaphase	Telophase
–Bio-Ro	57.7 ± 4.4	16.7 ± 5.8	25.7 ± 1.5
+Bio-Ro	9.0 ± 0	5.7 ± 1.2	85.3 ± 1.2
(with Bio-Ro/FITC-SA staining)	(0)	(0)	(62.3 ± 2.9)

Budding yeast wild-type (W3031A) cells in their exponential growth phase were incubated with Bio-Ro and stained with FITC-SA and DAPI as described in Experimental procedures (+Bio-Ro). The control cells (–Bio-Ro) were not incubated with Bio-Ro but subjected to the other procedures just as the Bio-Ro-treated cells were. The percentages of anaphase, metaphase and telophase cells within large-budded cells were judged as in Fig. 1(I) (n = 100). In Bio-Ro-treated large-budded cells, the percentages of the cells that had Bio-Ro/FITC-SA staining at the bud neck are given in parentheses. Note that all the large-budded cells with Bio-Ro/FITC-SA staining at the bud neck had segregated nuclei (telophase). Values are means ± SEM from three independent experiments.

incubation with Bio-Ro (25.7% without Bio-Ro) and that the cells with Bio-Ro/FITC-SA staining reached 62.3% of the total cell population with large bud (Table 1). These results suggest that the cell cycle progression was trapped at telophase by Bio-Ro treatment. In addition, the arrested cells at the S phase or mitotic metaphase were more viable than the growing cells after a 3-h incubation with Ro (Fig. 2B), probably reflecting lesser PE exposure in the arrested cells. The results in Fig. 2 also imply that PE exposure is not simply because of the membrane curvature at the bud neck.

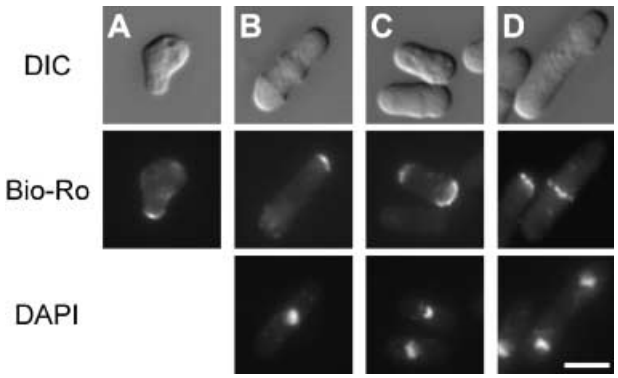

Figure 3 Yeast cells were stained with Bio-Ro at the polarized ends. (A) Exponentially growing budding yeast wild-type (W3031A) cells were incubated with 4 μg/mL α_1-mating factor acetate salt hydrate (Sigma) for 3 h and treated with 100 μM Bio-Ro and 4 μg/mL α_1-mating factor for an additional 3 h. After fixation, the spheroplasts were incubated with DAPI and FITC-SA as described in Experimental procedures. A representative DIC image (upper) and a Bio-Ro/FITC-SA staining image (lower) are shown. (B–D) Exponentially growing fission yeast wild-type (972) cells were treated with 100 μM Bio-Ro for 3 h. After fixation, the spheroplasts were incubated with DAPI and FITC-SA as described in Experimental procedures. Each panel contains a DIC image (upper), a Bio-Ro/FITC-SA staining image (middle) and a DAPI staining image (lower). Bar, 5 μm.

Bio-Ro/FITC-SA staining was observed at the polarized ends in yeast cells

Bio-Ro/FITC-SA-stained sites described above are the polarized ends at a specific stage of the cell division cycle, where the plasma membrane is extended and organized. To further confirm this correlation, the growing end of the mating projection, the shmoo, was tested for Bio-Ro/FITC-SA staining. The fluorescence was observed at the tip of the shmoo (Fig. 3A). These findings strongly suggest that PE is exposed on the surface of the plasma membrane at the polarized ends.

We next tested for Bio-Ro/FITC-SA staining in fission yeast *Sc. pombe*, which differs greatly from *S. cerevisiae* in terms of its modes of cell division and cellular growth. After separation of the dividing *Sc. pombe* cells, the old end first grows and then, at a point in time known as NETO (new-end take-off) in the G_2 phase, the new end, located at the previous site of cytokinesis, starts to grow. Growth at both cellular ends ceases prior to mitosis and then septum formation is initiated during mitosis (Hayles & Nurse 2001; Yarm *et al.* 2001). Bio-Ro/FITC-SA staining was observed at the division plane of telophase cells in *Sc. pombe* (Fig. 3D), suggesting that PE exposure at the cell division site in late mitosis is conserved. Furthermore, Bio-Ro/FITC-SA staining was also observed at one end (Fig. 3B) or at both ends (Fig. 3C) of mono-nucleated *Sc. pombe* cells. These sites are quite consistent with the cellular growing sites of

fission yeast. Therefore, PE exposure at the polarized ends seems to be a common phenomenon among phylogenetically distant yeasts.

Ro treatment caused aberrant F-actin accumulation at the Bio-Ro/FITC-SA staining sites

All the observed Bio-Ro/FITC-SA-stained sites (i.e. the bud neck, the presumptive bud site, the emerging small bud cortex and the tip of the mating projection of *S. cerevisiae*; and the division plane and growing ends of *Sc. pombe*) are also well known as sites for the polarized assembly of the actin cytoskeleton (Pruyne & Bretscher 2000a,b; Yarm *et al.* 2001; Nelson 2003). Furthermore, treatment with Bio-Ro seemed to have blocked the cell cycle progression of *S. cerevisiae* cells at the early stage of bud emergence and at telophase, as described above. Therefore, it is plausible that PE exposure on the plasma membrane is an event that is in some manner related to the polarized organization of the actin cytoskeleton and cell polarity.

Ro promotes the binding of other Ro molecules to PE by inducing transbilayer lipid translocation (Makino *et al.* 2003). To examine the effects of the entrapment of surface-exposed PE and the enhancement of the amount of exposed PE on the actin cytoskeleton, we treated *S. cerevisiae* cells with Ro during the exponential growth phase and also during the formation of the mating projection. In Ro-untreated cells, actin patches formed normally and they showed polarized distribution, as previously described (Fig. 4A,D) (Pruyne & Bretscher 2000a,b; Yarm *et al.* 2001). However, in the Ro-treated cells, aberrant F-actin accumulation was observed at sites undergoing the polarized assembly of the actin cytoskeleton, i.e. the bud neck (Fig. 4C; arrow), the small bud (Fig. 4B,C; arrowhead) and the tip of the shmoo (Fig. 4E,F; arrowhead). As the sites with aberrant F-actin accumulation were close to those with Bio-Ro/FITC-SA staining, the binding of Ro to PE exposed on the surface of the plasma membrane may have led to an inhibition of the disassembly of F-actins at those sites or to an enhancement of accumulation and/or the assembly of actins. Therefore, the surface exposure of PE is likely involved in the regulation of actin cytoskeleton organization at polarized growth sites and at the cell division site in yeast cells.

Loss of Ros3p, Dnf1p or Dnf2p caused anomalous Bio-Ro/FITC-SA staining pattern

In *S. cerevisiae*, Ros3p and two P-type ATPases, Dnf1p and Dnf2p, were proposed to be involved in the inward-directed transbilayer translocation of PE across the plasma membrane (Kato *et al.* 2002; Pomorski *et al.* 2003). Ros3p is an evolutionarily conserved protein and has two paralogues, Cdc50p and Ynr048wp (Kato *et al.* 2002). Dnf1p and Dnf2p belong to Drs2p-related P-type ATPase family, which also includes Dnf3p and Neo1p (Pomorski *et al.* 2003). Among these proteins, Ros3p, Dnf1p and Dnf2p were known to localize in the plasma membrane (Kato *et al.* 2002; Kumar *et al.* 2002; Misu *et al.* 2003; Pomorski *et al.* 2003; Saito *et al.* 2004). Therefore, we constructed single null mutants as well as the combinatorial double and triple mutants of the genes encoding these three proteins, to examine whether they are involved in the retrieval of exposed PE from the outer leaflet of the plasma membrane.

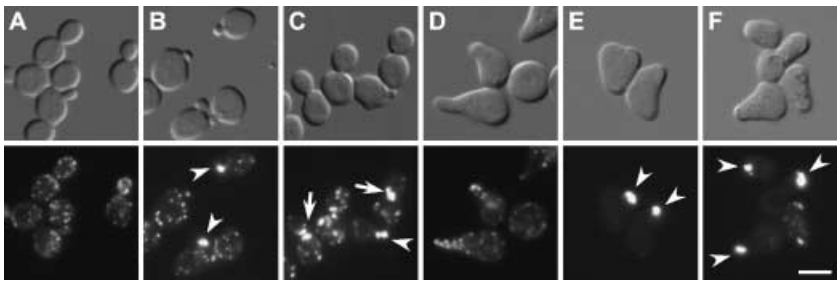

Figure 4 The actin cytoskeleton was affected by Ro treatment. Budding yeast wild-type (W3031A) cells were harvested during their exponential growth phase (A–C). The cells were then treated with Ro for 3 h at a final concentration of 0 μM (A), 15 μM (B) or 30 μM (C); the cells were fixed and labelled with rhodamine-phalloidin, as described in Experimental procedures. Exponentially growing W3031A cells were incubated with 4 μg/mL α_1-mating factor acetate salt hydrate (Sigma) for 3 h and treated with α_1-mating factor and 0 μM (D), 15 μM (E) or 30 μM (F) Ro for an additional 3 h. The cells were then fixed and labelled with rhodamine-phalloidin, as described in Experimental procedures. A DIC image (upper) and a rhodamine-phalloidin staining image (lower) are shown in each panel. Large aberrant F-actin structures were observed at the small bud (B,C; arrowhead), at the bud neck of the large-budded cells (C; arrow) and at the tip of the mating projection (E,F; arrowhead). Bar, 5 μm.

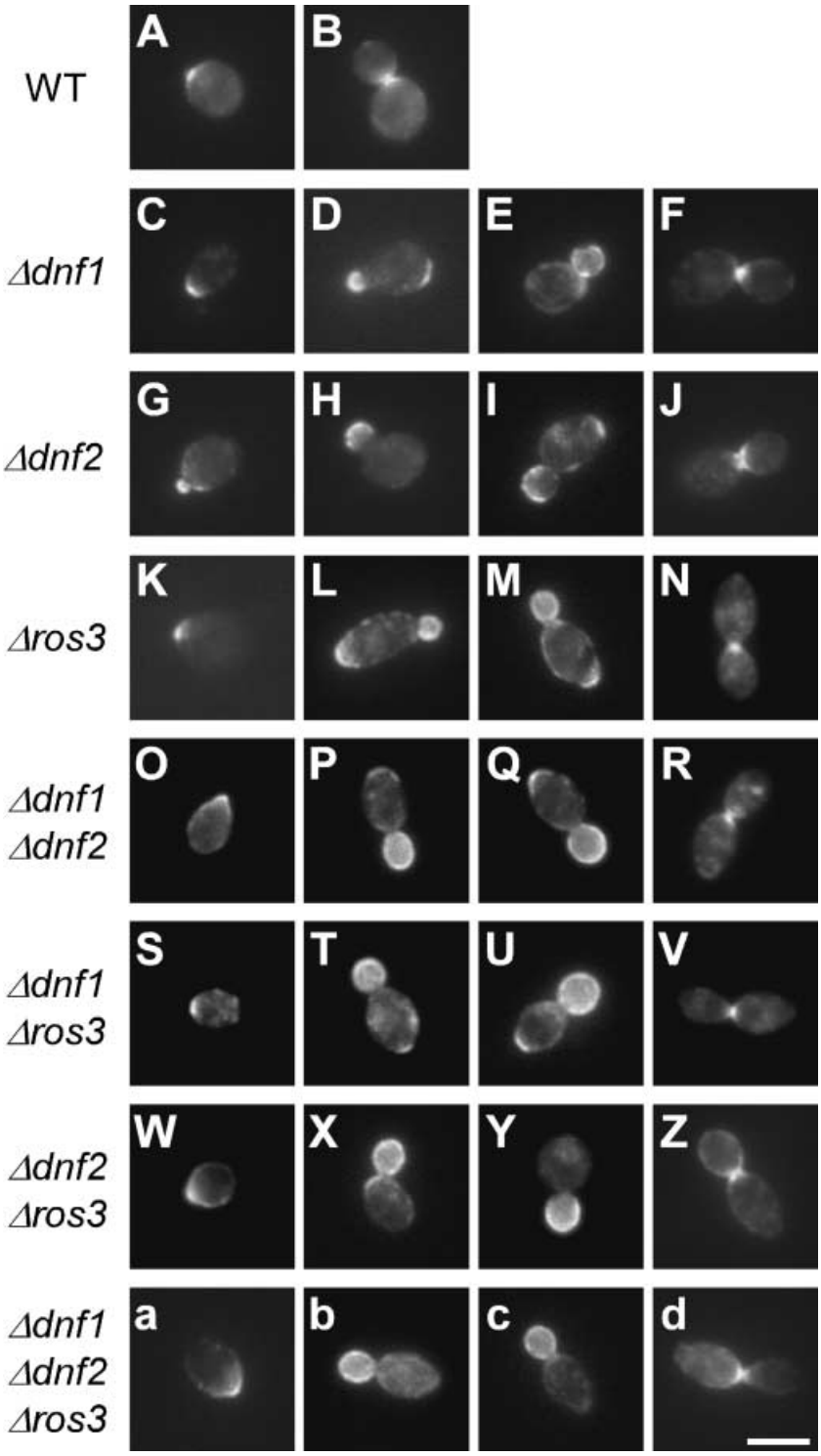

Figure 5 *Δros3*, *Δdnf1* and *Δdnf2* single and the combinatorial mutants showed anomalous Bio-Ro/FITC-SA staining pattern. Exponentially growing budding yeast wild-type (W3031A; A,B), *Δdnf1* (SKY001; C–F), *Δdnf2* (SKY002; G–J), *Δros3* (SKY003; K–N), *Δdnf1Δdnf2* (SKY004; O–R), *Δdnf1Δros3* (SKY005; S–V), *Δdnf2Δros3* (SKY006;W–Z) and *Δdnf1Δdnf2Δros3* (SKY007; a–d) cells were treated with Bio-Ro for 3 h. After fixation, the spheroplasts were incubated with FITC-SA as described in Experimental procedures. A Bio-Ro/FITC-SA staining image is shown in each panel. Bar, 5 μm.

In these mutants, Bio-Ro/FITC-SA staining was observed at the presumptive bud site, at the emerging small bud cortex and at the bud neck of the large-budded cells (Fig. 5C,F,G,J,K.N,O,R,S,V,W,Z,a,d), as in wild-type (Fig. 5A,B). The mutant cells that were stained with Bio-Ro at their bud neck completed nuclear segregation, as wild-type cells (data not shown). Furthermore, Bio-Ro/FITC-SA staining was also observed at the

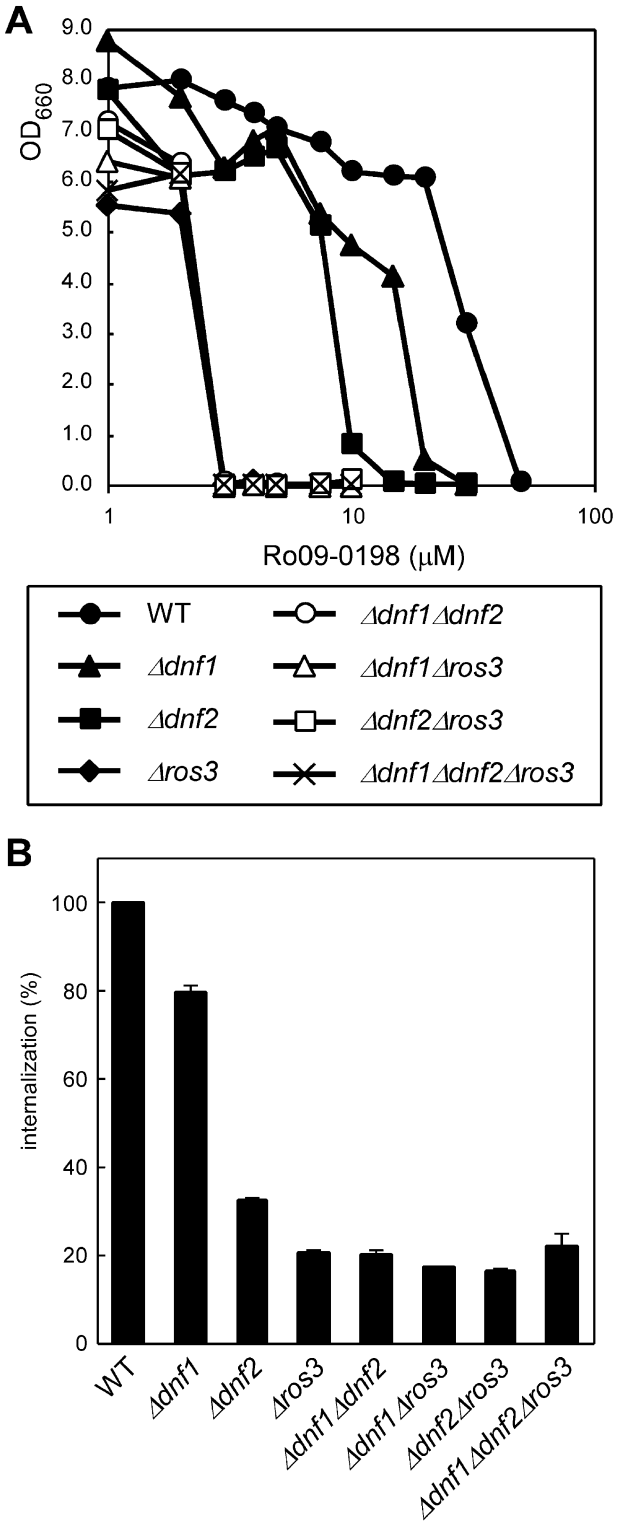

Figure 6 Effects of combinatorial deletion of *ROS3*, *DNF1* and *DNF2*. (A) Budding yeast wild-type (W3031A), *Δdnf1* (SKY001), *Δdnf2* (SKY002), *Δros3* (SKY003), *Δdnf1Δdnf2* (SKY004), *Δdnf1Δros3* (SKY005), *Δdnf2Δros3* (SKY006) and *Δdnf1Δdnf2Δros3* (SKY007) cells were diluted to an initial OD660 of 0.05 and then were incubated with YPD medium containing various concentrations of Ro and incubated for 48 h at 30 °C. OD_{660} values were measured after the incubation. (B) Yeast cells were harvested during their exponential growth phase and incubated with M-C_6-NBD-PE-containing vesicles for 30 min. Internalization of M-C_6-NBD-PE was measured by flow cytometry, as described in Experimental procedures. Data represent the percentages of fluorescent intensity relative to wild-type cells and values are means ± SEM from three independent experiments.

enlarging bud cortex (i.e. the bud cortex of the small-, medium- and large-budded cells) in these mutants (Fig. 5D,E,H,I,L,M,P,Q,T,U,X,Y,b,c). Most of the mutant cells with Bio-Ro/FITC-SA staining at the enlarging bud cortex did not complete nuclear segregation (data not shown). These observations suggest that PE is still exposed on the cell surface at the enlarging bud cortex in these mutants, and that Dnf1p, Dnf2p and Ros3p are involved in the transbilayer translocation of exposed PE to the inner leaflet at the bud cortex. This is consistent with the previous observation that Dnf1p and Dnf2p particularly localized at the small bud cortex and emerging bud sites (Pomorski *et al.* 2003). The mutant cells with Bio-Ro/FITC-SA-stained enlarging bud were often stained at the distal end of the mother cell (Fig. 5D,I,L,M,P,Q,T,U). This staining might be an indicative of abnormality of polarization in the mutant cells. It should be noted that Bio-Ro/FITC-SA staining was not observed at the mother cell cortex except the distal end and at the large bud cortex of the late mitotic cells, suggesting that the other system(s) that retain PE in the inner leaflet of the plasma membrane remain.

Δros3 and *Δdnf1Δdnf2* mutants were reported to be more sensitive to Ro than the wild-type (Kato *et al.* 2002; Pomorski *et al.* 2003). To compare the Ro sensitivity among the above mutants, they were incubated with various concentrations of Ro. *Δdnf1* and *Δdnf2* single mutants were sensitive to Ro and *Δdnf1Δdnf2* mutant was much more sensitive to Ro than the single mutants (Fig. 6A). *Δros3* mutant and *Δdnf1Δdnf2* mutant were similarly sensitive to Ro and the combination of *Δros3* with *Δdnf1* and/or *Δdnf2* did not confer further sensitivity to Ro (Fig. 6A). These results coincide well with extents of defective internalization of fluorescence-labelled PE by these mutants (Fig. 6B). Taken together with the report that Dnf1p and Dnf2p are highly similar in their structure and localization (Pomorski *et al.* 2003), they are likely functionally redundant and, furthermore, Ros3p seems to function in the same pathway as Dnf1p and Dnf2p.

Discussion

The involvement of local PE-exposed domains in cell polarity

In this study, we investigated Bio-Ro/FITC-SA staining in budding yeast *S. cerevisiae* and in fission yeast *Sc. pombe*. Our results indicated that PE is exclusively exposed on the surface of the plasma membrane at specific sites during specific stages of the cell division cycle (Fig. 7). The observed staining might also represent an enhanced signal, because Ro and Bio-Ro promote the binding of other Ro and Bio-Ro molecules to the membrane by inducing transbilayer lipid translocation (flip-flop) (Makino *et al.* 2003). While the binding of Ro to PE was not dependent on incubation temperature, Ro neither induced flip-flop nor showed cytotoxicity at 4 °C (Makino *et al.* 2003). When treated with Bio-Ro at 4 °C, *S. cerevisiae* wild-type cells were stained with Bio-Ro at the presumptive bud site (Fig. 1L) and at the bud neck of the large-budded cells (Fig. 1M), although the fluorescence was extremely weak and the ratio of the cells with Bio-Ro/FITC-SA staining was low. These observations suggest that PE is initially exposed at the same sites where Bio-Ro bound at 25 °C.

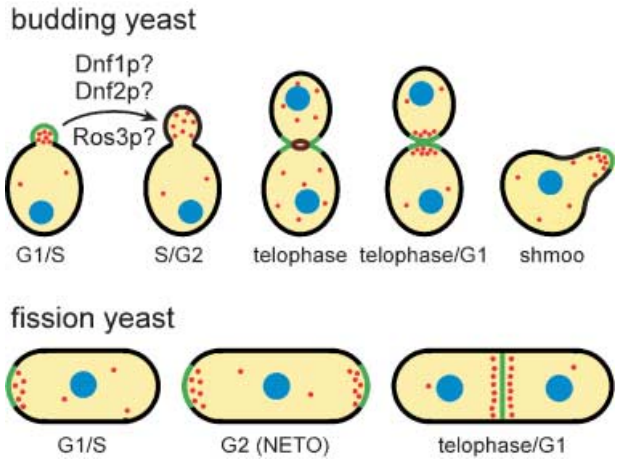

Figure 7 Schematic involvement of limited surface exposure of PE in cell polarity. PE would be exposed on the outer leaflet of the plasma membrane at the polarized ends (green), i.e. the presumptive bud site, the emerging small bud cortex, the bud neck of the late mitotic large-budded cells and the tip of the shmoo in budding yeast, and the tips of growing cell ends and the division plane of the late mitotic cells in fission yeast. These are the sites of the polarized assembly of the actin cytoskeleton at which the actomyosin ring (brown) is organized or actin patches (red) accumulate. PE exposure within the limited area described here is likely to be involved in the organization of the polarized actin cytoskeleton. PE exposure at the cell division site would occur after the segregation of the nuclei (blue). Ros3p, Dnf1p and Dnf2p are likely to be involved in the retrieval of exposed PE at the bud cortex following the initial stage of bud emergence.

We observed Bio-Ro/FITC-SA staining at the division site in yeast and also observed aberrant F-actin accumulation at the bud neck in Ro-treated *S. cerevisiae* large-budded cells. These observations seem to represent phenomena parallel to the FL-SA-Ro staining and the inhibition of contractile ring disassembly at the cleavage furrow in CHO cells (Emoto *et al.* 1996; Emoto & Umeda 2000). Therefore, PE exposure at the division site and its implications for the organization of the actin cytoskeleton are likely widely conserved mechanisms among eukaryotes. However, it remains uncertain whether or not the observed aberrant F-actin structure at the bud neck is equivalent to the contractile ring of CHO cells. The actomyosin contractile ring is also present at the bud neck (Fig. 7) (Field *et al.* 1999) and is crucial for cytokinesis in *S. cerevisiae* (Tolliday *et al.* 2002; 2003). As the actin ring is a dynamic structure as a result of the rapid turnover of actins (Tolliday *et al.* 2002), it is likely that the aberrant F-actin accumulation observed here was caused by an inhibition of the disassembly of the actin ring. Alternatively, actin patches accumulate at the bud neck following cytokinesis (Fig. 7) (Pruyne & Bretscher 2000a). Thus, it is also possible that the aberrant actin structure at the bud neck reflected some abnormality in the organization of the actin patches.

In addition to the staining at the cell division site, we observed Bio-Ro/FITC-SA staining at the presumptive bud site, at the emerging small bud cortex and at the tip of the shmoo in *S. cerevisiae*, as well as at the tips of growing cell ends in *Sc. pombe*. These sites are all well known to be the polarized ends at which actin patches accumulate and actin cables converge (Pruyne & Bretscher 2000a,b; Yarm *et al.* 2001; Nelson 2003). Therefore, PE would be exclusively exposed on the surface of the plasma membrane at such polarized ends (the cell division site is also a polarized end in yeast cells) (Fig. 7). Furthermore, we also observed aberrant F-actin accumulation at the small bud and at the tip of the shmoo in *S. cerevisiae* cells when the cells had been treated with Ro. This type of aberrant F-actin accumulation seems to be reflective of an abnormality in the organization of actin cables or actin patches. Actin cables are known to be tracks for the myosin-dependent polarized transport of vesicles and cargos in budding yeast (Pruyne & Bretscher 2000b; Nelson 2003). Alternatively, actin patches are thought to be involved in the endocytic process and in the enhancement and maintenance of cell polarity (Pruyne & Bretscher 2000b; Kaksonen *et al.* 2003). The actin cytoskeleton at the cell cortex is also believed to be

important in local vesicle delivery in higher eukaryotes (Pruyne & Bretscher 2000b; Nelson 2003). Therefore, it is plausible that PE influences cell polarity by controlling the organization of the actin cytoskeleton at the cell cortex. Based on the present results, we hypothesized that PE exposure on the plasma membrane in these specialized areas is involved in the dynamic organization of the actin cytoskeleton, not only at the cell division site, but more generally at cellular polarized ends (Fig. 7). Moreover, this hypothesis also accounts for a previous observation in which streptavidin-conjugated Bio-Ro (SA-Ro)-treated NIH3T3 cells lost actin stress fibres and instead showed aberrantly accumulated F-actins proximal to areas of SA-Ro cell-surface staining (Umeda & Emoto 1999). It remains to be determined how PE interacts with the machinery that controls the polarized organization of the actin cytoskeleton.

The formation and the disappearance of PE-exposed domains

Because Bio-Ro/FITC-SA staining was observed during a limited period of the cell cycle in *S. cerevisiae* wild-type cells and PE exposure was not likely due to membrane curvature, some cellular processes should be involved in the formation and the disappearance of limited PE-exposed domains. The formation of these domains is likely accompanied by the departure from equilibrium that PE mainly resides in the inner leaflet of the plasma membrane. It is plausible that such PE exposure is as a result of outward PE translocation within the limited area. It is also possible that PE-exposed domains are produced by lateral concentration of PE in the outer leaflet or a supply of PE to the outer leaflet of the plasma membrane by secretory vesicle fusion.

In the case of the disappearance of PE-exposed domains, PE would be retrieved from the outer leaflet of the plasma membrane immediately after the bud emergence. Ros3p and two P-type ATPases, Dnf1p and Dnf2p, have been proposed to participate in the inward PE translocation of the budding yeast plasma membrane (Kato *et al.* 2002; Pomorski *et al.* 2003). In the *ros3*, *dnf1* and *dnf2* single null mutant cells as well as the combinatorial double and triple mutant cells, we also observed Bio-Ro/FITC-SA staining at the enlarging bud cortex, which were not observed in wild-type cells. These results suggest that Ros3p, Dnf1p and Dnf2p are involved in the retrieval of exposed PE from the outer leaflet of the plasma membrane at the bud cortex after the initial stage of bud emergence. This is consistent with the previous observation that Dnf1p and Dnf2p particularly localized at the small bud cortex and emerging bud sites (Pomorski *et al.* 2003). Dnf1p also localize at the bud neck of dividing cells (Saito *et al.* 2004).

As *Δdnf1Δdnf2* mutant showed higher sensitivity to Ro and severer defects in internalization of fluorescence-labelled PE than *Δdnf1* and *Δdnf2* single mutants, and Dnf1p and Dnf2p are reported to be highly similar in their structure and localization (Pomorski *et al.* 2003), they are likely functionally redundant. In contrast, *Δros3*, the double and the triple mutants showed almost the same sensitivity to Ro, similar defects in internalization of fluorescence-labelled PE and the same Bio-Ro/FITC-SA staining pattern, implying that Ros3p functions in the same pathway as Dnf1p and Dnf2p. As Ros3p shows no significant homology with ABC transporters or P-type ATPases (Kato *et al.* 2002), Ros3p might have a regulatory function for Dnf1p and Dnf2p. Indeed, association of Ros3p with Dnf1p was suggested (Saito *et al.* 2004). In the single, double and triple mutants, the mother cortex, except the distal end and the bud cortex of the late mitotic cells, was not stained with Bio-Ro, indicating that there should be some alternative system(s) that contribute to the asymmetric distribution of PE in the plasma membrane.

The yeast system reported in this study would be very useful in revealing the underlying molecular mechanisms that account for how a PE exposed-domain is formed and regulated and how PE controls the polarized organization of the actin cytoskeleton.

Experimental procedures

Strains, materials and media

Yeast strains used in this study are listed in Table 2. Ro was kindly provided by H. Ishitsuka (Nippon Roche Research Center, Japan). Ro was also purified from the culture medium of *Streptoverticillium griseoverticillatum* NAR164C-MY6 strain (ATCC) as described in Takemoto *et al.* (1984) United States Patent 4,452,782. Ro was biotinylated as previously described (Makino *et al.* 2003). Unless otherwise indicated, yeast cells were grown at 25 °C in YPD medium, composed of 1% yeast extract (Difco Laboratories), 2% polypeptone (Nihon Seiyaku) and 2% glucose. To avoid the vacuolar fluorescence in the *ade2* genetic background, YPD medium was supplemented with adenine at a final concentration of 200 μg/mL.

Fluorescence microscopy

To stain yeast cells with Bio-Ro, 5×10^5 cells in the exponential growth phase were harvested, suspended in 5 μL YPD medium containing 100 μM Bio-Ro and incubated for 3 h at 25 °C, unless otherwise indicated. The cells were washed with phosphate-buffered saline (PBS) and fixed with PBS containing 5% (v/v) formaldehyde for 1 h at 30 °C. The cells were then washed with 100 μL PBS two times and with 100 μL spheroplasting buffer [100 mM HEPES-KOH (pH 7.2), 1 M sorbitol and 5 mM NaN_3]. The

Table 2 Yeast strains used in this study

Strain	Genotype	Source
W3031A	*MATa ade2-1 ura3-1 his3-11, 15 trp1-1 leu2-3, 112 can1-100*	ATCC
SKY001	*MATa ade2-1 ura3-1 his3-11, 15 trp1-1 leu2-3, 112 can1-100 Δdnf1::LEU2*	This study
SKY002	*MATa ade2-1 ura3-1 his3-11, 15 trp1-1 leu2-3, 112 can1-100 Δdnf2::HIS3*	This study
SKY003	*MATa ade2-1 ura3-1 his3-11, 15 trp1-1 leu2-3, 112 can1-100 Δros3::TRP1*	This study
SKY004	*MATa ade2-1 ura3-1 his3-11, 15 trp1-1 leu2-3, 112 can1-100 Δdnf1::LEU2 Δdnf2::HIS3*	This study
SKY005	*MATa ade2-1 ura3-1 his3-11, 15 trp1-1 leu2-3, 112 can1-100 Δdnf1::LEU2 Δros3::TRP1*	This study
SKY006	*MATa ade2-1 ura3-1 his3-11, 15 trp1-1 leu2-3, 112 can1-100 Δdnf2::HIS3 Δros3::TRP1*	This study
SKY007	*MATa ade2-1 ura3-1 his3-11, 15 trp1-1 leu2-3, 112 can1-100 Δdnf1::LEU2 Δdnf2::HIS3 Δros3::TRP1*	This study
972	h^-	M.Yoshida

budding yeast fixed cells were suspended in 50 μL spheroplasting buffer containing 100 μg/mL Zymolyase 100T (Seikagaku Corp.) and were incubated for 10 min at 30 °C. The fission yeast fixed cells were suspended in 100 μL spheroplasting buffer containing 500 μg/mL Zymolyase 100T (Seikagaku Corp.) and 100 μg/mL Lysing enzymes from *Trichoderma harzianum* (Sigma) and were incubated for 15 min at 37 °C. The spheroplasts were attached to poly L-lysine-coated multiwell slides, fixed for 6 min in methanol and 30 s in acetone, both at −20 °C and incubated in PBS containing 0.1% (w/v) bovine serum albumin for 30 min at room temperature. After washing with FITC-SA buffer [10 mM phosphate (pH 7.8), 0.15 M NaCl] three times, Fluorescein Streptavidin (Vector Laboratories) incubation was carried out at a final concentration of 5 μg/mL in the FITC-SA buffer for 1 h at room temperature. In the last 10 min of the incubation, 4′,6-diamidino-2-phenylindole (DAPI) was added at the final concentration of 62.5 ng/mL. After washing with FITC-SA buffer three times, cells were observed and photographed using a photomicroscope (model BX52; Olympus). Images were acquired by a high-resolution digital charge-coupled device camera (model C4742-95–12ER; Hamamatsu Photonics) and processed by AquaCosmos software (ver. 2.0.1.1; Hamamatsu Photonics).

For the labelling of budding yeast cells with rhodamine-phalloidin after the incubation with Ro, 1×10^7 cells were harvested during the exponential growth phase. The cells were suspended in 200 μL YPD medium containing various concentrations of Ro and incubated for 3 h at 25 °C. After washing with 100 μL PBS, the cells were fixed with PBS containing 5% (v/v) formaldehyde for 1 h at 30 °C. After washing with 100 μL PBS three times, the cells were incubated with 200 μL PBS containing Rhodamine Phalloidin (Cytoskeleton Inc.) at the final concentration of 14 nM for 2 h at 30 °C. Cells were washed with 100 μL PBS three times, observed and photographed as described above.

Budding yeast cells were stained with filipin (Sigma) as previously described (Bagnat & Simons 2002).

Measurement of viable cells

Cell viability was measured by staining dead cells as follows. Budding yeast cells were washed with PBS and incubated with PBS containing 10 μM phloxine B (Sigma) for 5 min at room temperature. After washing the cells with PBS three times, dead cells were determined by phloxine B staining and flow cytometry. As controls for dead cells, wild-type (W3031A) cells were incubated for 30 min at 60 °C. Flow cytometric analysis was performed with a FACScan cytometer (Becton Dickinson) and CELLQuest software (ver. 3.1f; Becton Dickinson).

Internalization of fluorescence-labelled PE into cells

1-Myristoyl-2-{6-[(7-nitro-2-1,3-benzoxadiazol-4-yl)amino]-hexanoyl}-sn-glycero-3-phosphoethanolamine (M-C_6-NBD-PE; Avanti Polar Lipids Inc.) was purified by preparative TLC. Purified M-C_6-NBD-PE and 1-palmitoyl-2-oleoyl-sn-glycero-3-phosphocholine (Avanti Polar Lipids Inc.) were used for vesicle preparation. Measurement of M-C_6-NBD-PE internalization into yeast cells was carried out as previously described (Kato *et al.* 2002).

Plasmids and strain construction

The plasmids used in this study are pT-HIS3, pT-LEU2 and pT-TRP1 (Nikawa & Kawabata 1998). *dnf1*, *dnf2* and *ros3* deletion mutants (*Δdnf1*, *Δdnf2* and *Δros3*, respectively) were constructed in W3031A background as previously described (Nikawa & Kawabata 1998). The PCR primers used are listed in Table 3. The resultant deletion mutants were used for the transformation to construct the double and triple deletion mutants of these genes. The success of gene deletion was confirmed by PCR and Southern blot.

Acknowledgements

We are grateful to Minoru Yoshida (RIKEN, Saitama, Japan) and Hiroshi Taoka (the University of Tokyo, Tokyo, Japan) for the 972 strain and for technical help with it, to Jun-ichi Nikawa (Kyushu Institute of Technology, Fukuoka, Japan) for the plasmids, pT-HIS3, pT-LEU2 and pT-TRP1, to Kazuo Emoto (the Tokyo Metropolitan Institute of Medical Science, Tokyo, Japan) and Yoshihisa Shimizu (RIKEN, Saitama, Japan) for their valuable suggestions, and to Hidemitsu Nakamura (NIAS, Ibaraki, Japan)

Table 3 PCR primers used in this study

	Primer name	Sequence
For *DNF1* disruption	DNF1 A-f	5′-GAAGGTCATCGTAATACGCA-3′
	DNF1 A-r	5′-GGGCATATTGTAATACACAGTC-3′
	DNF1 B-f	5′-CTATTGCTGTAATTTCGTGT-3′
	DNF1 B-r	5′-TTGATGGATATTAGCGAATG-3′
	pT-LEU2-f	5′-ACTCAGGTATCGTAAGATGC-3′
	pT-LEU2-r	5′-CACGTTGAGCCATTAGTATC-3′
For *DNF2* disruption	DNF2 A-f	5′-GCCAGATTTTTACTAGACGCG-3′
	DNF2 A-r	5′-CTCAATATCATCCACGAAGGG-3′
	DNF2 B-f	5′-CAAGCTCGTCGTCAAGTAAC-3′
	DNF2 B-r	5′-AGCATCTCTTCTCTTGTGCG-3′
	pT-HIS3-f2	5′-CTTCATTCAACGTTTCCCATTG-3′
	pT-HIS3-r2	5′-CGCCTCGTTCAGAATGACACGT-3′
For *ROS3* disruption	YNL323A-f	5′-TGAGGACTATCGTAAAGAGAC-3′
	YNL323A-r	5′-CTCCTTTGTCCTTTCTACGG-3′
	YNL323B-f	5′-GGCGGTAGAAAGATTGCTGA-3′
	YNL323B-r	5′-TCCTCCAGTGTAAAGACGAC-3′
	pT-TRP1-f	5′-TTCACAGGTAGTTCTGGTCC-3′
	pT-TRP1-r	5′-GCAGGCAAGTGCACAAACAA-3′

for advice during the initial planning of this work. KI was a junior research associate of RIKEN. This work was supported in part by a grant-in-aid for scientific research from the Ministry of Education, Culture, Sports, Science and Technology of Japan. This work was performed by using the facilities of the Biotechnology Research Center of the University of Tokyo.

References

Aoki, Y., Uenaka, T., Aoki, J., Umeda, M. & Inoue, K. (1994) A novel peptide probe for studying the transbilayer movement of phosphatidylethanolamine. *J. Biochem. (Tokyo)* **116**, 291–297.

Bagnat, M. & Simons, K. (2002) Cell surface polarization during yeast mating. *Proc. Natl. Acad. Sci. USA* **99**, 14183–14188.

Bevers, E.M., Comfurius, P., Dekkers, D.W. & Zwaal, R.F. (1999) Lipid translocation across the plasma membrane of mammalian cells. *Biochim. Biophys. Acta* **1439**, 317–330.

Birner, R., Burgermeister, M., Schneiter, R. & Daum, G. (2001) Roles of phosphatidylethanolamine and of its several biosynthetic pathways in *Saccharomyces cerevisiae*. *Mol. Biol. Cell* **12**, 997–1007.

Choung, S.Y., Kobayashi, T., Inoue, J., *et al.* (1988a) Hemolytic activity of a cyclic peptide Ro09–0198 isolated from Streptoverticillium. *Biochim. Biophys. Acta* **940**, 171–179.

Choung, S.Y., Kobayashi, T., Takemoto, K., Ishitsuka, H. & Inoue, K. (1988b) Interaction of a cyclic peptide, Ro09–0198, with phosphatidylethanolamine in liposomal membranes. *Biochim. Biophys. Acta* **940**, 180–187.

Daleke, D.L. (2003) Regulation of transbilayer plasma membrane phospholipid asymmetry. *J. Lipid Res.* **44**, 233–242.

Decottignies, A., Grant, A.M., Nichols, J.W., *et al.* (1998) ATPase and multidrug transport activities of the overexpressed yeast ABC protein Yor1p. *J. Biol. Chem.* **273**, 12612–12622.

Dowhan, W. (1997) Molecular basis for membrane phospholipid diversity: why are there so many lipids? *Annu. Rev. Biochem.* **66**, 199–232.

Emoto, K. & Umeda, M. (2000) An essential role for a membrane lipid in cytokinesis. Regulation of contractile ring disassembly by redistribution of phosphatidylethanolamine. *J. Cell Biol.* **149**, 1215–1224.

Emoto, K., Kobayashi, T., Yamaji, A., *et al.* (1996) Redistribution of phosphatidylethanolamine at the cleavage furrow of dividing cells during cytokinesis. *Proc. Natl. Acad. Sci. USA* **93**, 12867–12872.

Field, C., Li, R. & Oegema, K. (1999) Cytokinesis in eukaryotes: a mechanistic comparison. *Curr. Opin. Cell Biol.* **11**, 68–80.

Grant, A.M., Hanson, P.K., Malone, L. & Nichols, J.W. (2001) NBD-labeled phosphatidylcholine and phosphatidylethanolamine are internalized by transbilayer transport across the yeast plasma membrane. *Traffic* **2**, 37–50.

Hayles, J. & Nurse, P. (2001) A journey into space. *Nat. Rev. Mol. Cell. Biol.* **2**, 647–656.

Heald, R. & Walczak, C.E. (1999) Microtubule-based motor function in mitosis. *Curr. Opin. Struct. Biol.* **9**, 268–274.

Ichimura, Y., Kirisako, T., Takao, T., *et al.* (2000) A ubiquitin-like system mediates protein lipidation. *Nature* **408**, 488–492.

Kaksonen, M., Sun, Y. & Drubin, D.G. (2003) A pathway for association of receptors, adaptors, and actin during endocytic internalization. *Cell* **115**, 475–487.

Kato, U., Emoto, K., Fredriksson, C., *et al.* (2002) A novel membrane protein, Ros3p, is required for phospholipid translocation across the plasma membrane in *Saccharomyces cerevisiae*. *J. Biol. Chem.* **277**, 37855–37862.

Kessler, H., Steuernagel, S. & Will, M. (1988) The structure or the polycyclic nonadecapeptide Ro 09–0198. *Helv. Chim. Acta* **71**, 1924–1929.

Kirisako, T., Ichimura, Y., Okada, H., *et al.* (2000) The reversible modification regulates the membrane-binding state of Apg8/

Aut7 essential for autophagy and the cytoplasm to vacuole targeting pathway. *J. Cell Biol.* **151**, 263–276.

Kumar, A., Agarwal, S., Heyman, J.A., *et al.* (2002) Subcellular localization of the yeast proteome. *Genes Dev.* **16**, 707–719.

Makino, A., Baba, T., Fujimoto, K., *et al.* (2003) Cinnamycin (Ro 09–0198) promotes cell binding and toxicity by inducing transbilayer lipid movement. *J. Biol. Chem.* **278**, 3204–3209.

Menon, A.K. & Stevens, V.L. (1992) Phosphatidylethanolamine is the donor of the ethanolamine residue linking a glycosylphosphatidylinositol anchor to protein. *J. Biol. Chem.* **267**, 15277–15280.

Misu, K., Fujimura-Kamada, K., Ueda, T., *et al.* (2003) Cdc50p, a conserved endosomal membrane protein, controls polarized growth in *Saccharomyces cerevisiae*. *Mol. Biol. Cell* **14**, 730–747.

Nelson, W.J. (2003) Adaptation of core mechanisms to generate cell polarity. *Nature* **422**, 766–774.

Nikawa, J. & Kawabata, M. (1998) PCR- and ligation-mediated synthesis of marker cassettes with long flanking homology regions for gene disruption in *Saccharomyces cerevisiae*. *Nucl. Acids Res.* **26**, 860–861.

Pomorski, T., Lombardi, R., Riezman, H., *et al.* (2003) Drs2p-related P-type ATPases Dnf1p and Dnf2p are required for phospholipid translocation across the yeast plasma membrane and serve a role in endocytosis. *Mol. Biol. Cell* **14**, 1240–1254.

Pruyne, D. & Bretscher, A. (2000a) Polarization of cell growth in yeast. I. Establishment and maintenance of polarity states. *J. Cell Sci.* **113**, 365–375.

Pruyne, D. & Bretscher, A. (2000b) Polarization of cell growth in yeast. II. The role of the cortical actin cytoskeleton. *J. Cell Sci.* **113**, 571–585.

Saito, K., Fujimura-Kamada, K., Furuta, N., *et al.* (2004) Cdc50p, a protein required for polarized growth, associates with the Drs2p P-type ATPase, implicated in phospholipid translocation in *Saccharomyces cerevisiae*. *Mol. Biol. Cell* **15**, 3418–3432.

Storey, M.K., Clay, K.L., Kutateladze, T., *et al.* (2001) Phosphatidylethanolamine has an essential role in *Saccharomyces cerevisiae* that is independent of its ability to form hexagonal phase structures. *J. Biol. Chem.* **276**, 48539–48548.

Takemoto, K., Miyasaka, Y., Ishitsuka, H., *et al.* (1984) Pentadecapeptide. US Patent 4, 452, 782.

Tolliday, N., VerPlank, L. & Li, R. (2002) Rho1 directs formin-mediated actin ring assembly during budding yeast cytokinesis. *Curr. Biol.* **12**, 1864–1870.

Tolliday, N., Pitcher, M. & Li, R. (2003) Direct evidence for a critical role of myosin II in budding yeast cytokinesis and the evolvability of new cytokinetic mechanisms in the absence of myosin II. *Mol. Biol. Cell* **14**, 798–809.

Umeda, M. & Emoto, K. (1999) Membrane phospholipid dynamics during cytokinesis: regulation of actin filament assembly by redistribution of membrane surface phospholipid. *Chem. Phys. Lipids* **101**, 81–91.

Yarm, F., Sagot, I. & Pellman, D. (2001) The social life of actin and microtubules: interaction versus cooperation. *Curr. Opin. Microbiol.* **4**, 696–702.

Zachowski, A. (1993) Phospholipids in animal eukaryotic membranes: transverse asymmetry and movement. *Biochem. J.* **294**, 1–14.

Received: 13 May 2004
Accepted: 22 July 2004